

# Consistent modeling of scalar transport in multiphase flows using conservative phase field methods

By S. Mirjalili, M. Khanwale AND A. Mani

## 1. Motivation and objectives

In recent years, phase field (diffuse interface) models have emerged as competitive alternatives to sharp-interface models for the simulation of two-phase flows (Mirjalili *et al.* 2017). This is owing to their simplicity in implementation, cost-efficiency, scalability, and regularity, allowing for the use of standard numerical methods (Mirjalili *et al.* 2019; Mirjalili & Mani 2021). Phase field methods belonging to the category of models based on the Cahn-Hilliard equation and second-order conservative phase field models are particularly attractive, as they enforce mass conservation on the continuous level (Jacqmin 1999; Abels *et al.* 2012; Shen & Yang 2010; Khanwale *et al.* 2020; Chiu & Lin 2011; Mirjalili *et al.* 2020; Huang *et al.* 2020). Additionally, it is often argued that phase field methods are desirable for modeling multi-physics effects because they (1) are modular, in the sense that new physical effects can be included simply by coupling to new equations without manipulating the numerical discretizations, and (2) increase the dimensionality of the interface, whereby all interfacial effects can be modeled volumetrically (Yue *et al.* 2004; Teigen *et al.* 2009; Liu *et al.* 2015; Soligo *et al.* 2019; Mirjalili *et al.* 2022). Crucially, any equation coupled to the phase field equation must consistently account for the conservative right-hand side (RHS) terms in the phase field equations. For instance, it is now well established that the momentum equations have to be modified to achieve the so-called mass-momentum consistency requirement that allows for robust simulations of high  $Re$  numbers and high density ratios (Zhu *et al.* 2019, 2020; Huang *et al.* 2020; Khanwale *et al.* 2020; Mirjalili & Mani 2021). Similarly, this work describes how consistency in scalar transport can be achieved when modeling two-phase flows with conservative phase field methods. Considering the equivalence between heat transport and dilute species mass transport, we use the term scalar to refer to both throughout this work (Mirjalili *et al.* 2022). As such, this work presents partial differential equations (PDEs) for consistent heat and mass transport in two-phase flows.

One-scalar models track a single scalar, such as heat content or species concentration per unit of total volume throughout the domain. Examples of such models for phase field methods are given by Zheng *et al.* (2015), Huang *et al.* (2021), and Mirjalili *et al.* (2022). One-scalar models typically suffer from artificial leakage and inaccurate results when the diffusivity ratio between the two phases is large or infinite (i.e., confined scalar). To address this problem, two-scalar models have been proposed in the literature for modeling two-phase systems with confined scalars (Jain & Mani 2020) and systems involving interphase scalar transfer (Mirjalili *et al.* 2022). The correction for consistency is presented here for both one-scalar and two-scalar models. Correction to the one-scalar model is briefly derived in Section 2 by making an analogy with momentum transport and inspecting the system at thermodynamic equilibrium. Next, we present how consistency

can be achieved for two-scalar models. A brief note on the computational schemes and positivity is given in Section 3. Then, we use numerical tests in Section 4 to verify our theoretical arguments and compare them against the inconsistent models. Finally, we summarize our findings and lay out future work to extend this report in Section 5.

## 2. Consistent scalar transport model

The equation for a conservative phase field model can be written as

$$\frac{\partial \phi}{\partial t} + \nabla \cdot (\vec{u}\phi) = \nabla \cdot \vec{R}, \quad (2.1)$$

where  $\phi$  is the phase field variable, with  $\phi = 1$  and  $\phi = 0$  representing the pure phases 1 and 2, respectively. In this work,  $\vec{R}$  is an arbitrary space- and time-varying function of  $\phi$  and its derivatives. Examples include models based on the original Cahn-Hilliard equation (Jacqmin 1999; Abels *et al.* 2012; Khanwale *et al.* 2020), models using degenerate mobility for the Cahn-Hilliard equation (Dai & Du 2016; Fu & Han 2021), and second-order conservative phase field equations (Chiu & Lin 2011; Mirjalili *et al.* 2020; Huang *et al.* 2020; Jain 2022).

Mirjalili *et al.* (2022) explained how the problems of heat transport and mass transport of a dilute species (i.e., negligible volume change from the presence of species) are equivalent. More specifically, in the physically realistic sharp interface situation, heat content—given by  $q = \rho C_p T$ , where  $\rho$ ,  $C_p$ , and  $T$  are density, specific heat capacity, and temperature, respectively—and species concentration per volume (denoted by  $c$ ) are conserved quantities governed by the advection-diffusion equations in the pure phases and boundary conditions at the interface. The diffusivity in phase  $i$  is denoted by  $D_i$ , and the jump in the scalar field across the interface is given by  $K_{\text{eq}}$ . For the case of mass transport,  $D_i$  is the species mass diffusivity in phase  $i$  and  $K_{\text{eq}}$  is the Henry coefficient, assumed to be a constant. It is defined as the concentration ratio in phase 1 to phase 2 upon reaching chemical equilibrium. For heat transport, the diffusivity of the heat content is  $D_i = k_i/(\rho_i C_{p,i})$ , where  $k_i$  is the thermal conductivity in phase  $i$ , and  $K_{\text{eq}} = (\rho_1 C_{p,1})/(\rho_2 C_{p,2})$  is the ratio of the heat capacities of phase 1 to 2, which is also the ratio of the heat contents upon reaching thermal equilibrium.

In the following subsection, we extend our previous work (Mirjalili *et al.* 2022) to introduce one-scalar and two-scalar models that account for an out-of-equilibrium interface ( $R \neq 0$ ).

### 2.1. One-scalar model

Assuming thermodynamic equilibrium at the interface (Mirjalili *et al.* 2022), the consistent one-scalar model is given by

$$\frac{\partial c}{\partial t} + \nabla \cdot (\vec{u}c) = \nabla \cdot \left[ D_{\text{eff}} \nabla \left( \frac{c}{K_{\text{eff}}} \right) \right] + \nabla \cdot \left[ \vec{R} (K_{\text{eq}} - 1) \frac{c}{K_{\text{eff}}} \right], \quad (2.2)$$

where  $c$  is the total heat or mass content per total volume, and where

$$D_{\text{eff}} = D_1 K_{\text{eq}} \phi + D_2 (1 - \phi) \quad (2.3)$$

and

$$K_{\text{eff}} = K_{\text{eq}} \phi + (1 - \phi) \quad (2.4)$$

are the effective mixture diffusivity and equilibrium concentration ratio across the interface, respectively. We note the addition of the last term on the RHS of Eq. (2.2) compared

to the one-scalar models presented in previous works (Zheng *et al.* 2015; Mirjalili *et al.* 2022). This term vanishes when  $K_{\text{eq}} = 1$  or when the interface is at equilibrium,  $\vec{R} = 0$ .

To outline the derivation of the consistency correction, let us inspect the consistent one-scalar model for the tangible case of heat transport, where Eq. (2.2) is equivalent to solving

$$\frac{\partial(\rho C_p)_{\text{eff}} T}{\partial t} + \nabla \cdot [\vec{u}(\rho C_p)_{\text{eff}} T] = \nabla \cdot (k_{\text{eff}} \nabla T) + \nabla \cdot [\vec{R}(\rho_1 C_{p,1} - \rho_2 C_{p,2}) T] \quad (2.5)$$

to obtain the temperature field, where

$$(\rho C_p)_{\text{eff}} = \rho_1 C_{p,1} \phi + \rho_2 C_{p,2} (1 - \phi) \quad (2.6)$$

and

$$k_{\text{eff}} = k_1 \phi + k_2 (1 - \phi) \quad (2.7)$$

are the effective mixture of heat capacity and conductivity, respectively. The last term in Eq. (2.5) is equivalent to the newly introduced last term on the RHS of Eq. (2.2). Intuitively, this term accounts for the fact that any flux in the RHS of the phase field equation changes the mixture's heat content locally when the heat capacities of the two phases is different. This is analogous to the correction used for mass-momentum consistency whereby any flux in the RHS of the phase field equation alters the mixture's momentum locally when the two phases have different densities. The last term in Eq. (2.5) enforces consistent transport of heat and volume fractions (mass), and it is only in the presence of this term that an isothermal equilibrium solution can be achieved on a continuous and discrete level. Essentially, upon thermal equilibrium (uniform  $T$ ), the heat transport equation becomes identical to the phase field equation. We acknowledge that other authors have also recently applied this correction for consistency to the energy equation; for example, Huang *et al.* (2022) in the context of incompressible gas-liquid-solid flows and Jain *et al.* (2020) in the context of compressible flows. To the best of our knowledge, though, consistent one-scalar models for mass transport have not been explored yet. In any case, the general consistent one-scalar model given by Eq. (2.2) applies to both heat and mass transport and is critical in most practical flows wherein  $K_{\text{eq}} \neq 1$ .

One-scalar models have been shown to yield accurate results when the diffusivity ratio between the two phases is moderate. For large and infinite (e.g., confined mass or heat-insulated phase) diffusivity ratios, two-scalar models are necessary to prevent artificial leakage (Davidson & Rudman 2002; Bothe & Fleckenstein 2013; Jain & Mani 2020; Mirjalili *et al.* 2022). A consistent two-scalar model that accounts for out-of-equilibrium interfaces is presented next.

## 2.2. Two-scalar model

Let us define  $c_i$  as the amount of scalar in phase  $i$  per unit total volume. In the absence of interfacial transfer,  $c_i$  are conserved variables. For two-phase flows, the consistent two-scalar model is given by

$$\frac{\partial c_1}{\partial t} + \nabla \cdot (\vec{u} c_1) = \nabla \cdot \left[ D_1 \phi \nabla \left( \frac{c_1}{\phi} \right) \right] + J + \nabla \cdot \left( \vec{R} \frac{c_1}{\phi} \right), \quad (2.8)$$

$$\frac{\partial c_2}{\partial t} + \nabla \cdot (\vec{u} c_2) = \nabla \cdot \left[ D_2 (1 - \phi) \nabla \left( \frac{c_2}{1 - \phi} \right) \right] - J + \nabla \cdot \left( -\vec{R} \frac{c_2}{1 - \phi} \right), \quad (2.9)$$

where the interphase transfer term,  $J$ , is given by

$$J = AD_m [K_{\text{eq}} c_2 \phi - c_1 (1 - \phi)] - D_m \nabla \phi \cdot \nabla (c_1 + K_{\text{eq}} c_2), \quad (2.10)$$

and the mixture diffusivity,  $D_m$ , is

$$D_m = \frac{D_1 D_2}{K_{\text{eq}} D_1 (1 - \phi) + D_2 \phi}. \quad (2.11)$$

In Eq. (2.10), there is a free parameter,  $A$ , which represents the inverse timescale to thermodynamic equilibrium, typically chosen to be a large constant, without imposing additional time-step restrictions. The interphase transfer term,  $J$ , is the same as what was derived and used by Mirjalili *et al.* (2022). For the reader's convenience, we give the two-scalar model from Mirjalili *et al.* (2022) here, where

$$\frac{\partial c_1}{\partial t} + \nabla \cdot (\vec{u} c_1) = \nabla \cdot \left[ D_1 \left( \nabla c_1 - \frac{1 - \phi}{\epsilon} \vec{n} c_1 \right) \right] + J, \quad (2.12)$$

$$\frac{\partial c_2}{\partial t} + \nabla \cdot (\vec{u} c_2) = \nabla \cdot \left[ D_2 \left( \nabla c_2 + \frac{\phi}{\epsilon} \vec{n} c_2 \right) \right] - J. \quad (2.13)$$

Comparing Eqs. (2.8)–(2.9) to Eqs. (2.12)–(2.13), we notice two modifications. First, the diffusion within each phase [the first terms on the RHS of Eqs. (2.8)–(2.9)] is modeled by  $\nabla \cdot [D_1 \phi \nabla (c_1/\phi)]$  and  $\nabla \cdot [D_2 (1 - \phi) \nabla (c_2/(1 - \phi))]$ , respectively. This eliminates the error committed by Jain & Mani (2020) and Mirjalili *et al.* (2022) associated with assuming phase field equilibrium for the second-order conservative phase field method ( $\vec{R} = 0$ ) when deriving diffusion within each phase [the first terms on the RHS of Eqs. (2.12)–(2.13)]. In fact, Mirjalili *et al.* (2022) derived these inconsistent terms starting from the terms used in Eqs. (2.8)–(2.9). Second, the last terms on the RHS of Eqs. (2.8)–(2.9) account for the scalar transport due to the RHS of the phase field model. Formal derivation of these corrective terms is deferred to a future publication on this topic. To explain the consistency briefly, upon reaching thermodynamic equilibrium, regardless of the phase field equation, the two-scalar models attain steady and spatially uniform values for  $c_1/\phi = K_{\text{eq}} c_2/(1 - \phi) = \text{const.}$ , which cause the first two terms on the RHS of Eqs. (2.8)–(2.9) to vanish. Setting aside scaling constants, these two equations would be identical to the phase field equation. Hence, the scalars would simply be advected with a modified advection velocity which is identical to what advects  $\phi$ .

Note that to avoid 0/0, a very small number must be added to the numerator and denominator when computing  $c_1/\phi$  and  $c_2/(1 - \phi)$ . Note also that to achieve positivity of the scalar concentrations, the time step must be reduced by a factor of two compared to the model given by Mirjalili *et al.* (2022). Proof of this is also deferred to future work.

In addition to consistently accounting for the RHS of the phase field equation, the proposed two-scalar model in this work achieves all the consistency conditions of its predecessor (Mirjalili *et al.* 2022): (1) conservation, (2) generalizability (i.e., heat versus mass, arbitrary diffusivity ratios), (3) reduction consistency for confined scalars (Jain & Mani 2020) when either diffusivity is zero, (4) reduction consistency to bulk equations away from interfaces, (5) accuracy in predicting long-time equilibrium solutions, and (6) prevention of unphysical leakage in the practical limit of large diffusivity ratios. Moreover, the model in Eqs. (2.8)–(2.9) is valid and accurate regardless of the form of  $\vec{R}$ , whereas the accuracy of Eqs. (2.12)–(2.13) depends on the equilibrium of the interface and, for instance, results in significant leakage when coupled to the Cahn-Hilliard equation. In the following, we demonstrate the importance of consistently accounting for the phase field RHS terms in the PDEs for scalar transport using simple numerical tests.

### 3. Computational approach and positivity

We use one-dimensional (1D) numerical tests to assess the accuracy and importance of the consistent PDE models we have introduced. Since we focus on assessing and comparing PDE models, we use standard numerical methods in space and time. We solve the phase field equation coupled to the scalar transport equations while using a prescribed constant value for velocity,  $\vec{u}$ . For simplicity, explicit Euler is used for time integration. This is permitted because the stiffness of the phase field equations is typically dominated by the diffusion terms (Mirjalili *et al.* 2020) rather than hyperbolic advective effects. In space, second-order central finite difference spatial discretization is used on a standard staggered Cartesian grid where velocity vectors and all fluxes, including the scalar fluxes, are stored on the faces, while scalar concentrations and the phase field variable are stored on cell centers. We refer to Mirjalili *et al.* (2020) for a more detailed description of the computational algorithm (without scalar transport). As briefly mentioned in Section 2.2, to guarantee positivity of  $c_1 + c_2$  and stability for the two-scalar model, the time step should be reduced by a factor of two compared to the two-scalar model presented by Mirjalili *et al.* (2022). Specifically, for a small enough mesh spacing,  $\Delta x \leq 2 \min(D_1, D_2)/|\vec{u}|_{max}$ , the positivity of  $c_1 + c_2$  is guaranteed as long as  $\Delta t \leq \Delta x^2/[4D_f \max(D_1, D_2)]$ , where  $D_f$  is the number of spatial dimensions, and  $\Delta t$  is the time step size. These requirements are most relevant when the diffusivity ratio is large or infinite (i.e., confined scalar). We will formally derive these conditions in future work.

### 4. Numerical tests

Here, we present two proof-of-concept 1D tests for different phase field models coupled with various options for scalar transport to demonstrate the importance of consistently accounting for the phase field RHS terms in the PDEs for scalars. Both tests use a constant value of  $\vec{u} = 1$  to advect everything in a periodic domain of  $[-1, 1]$ , discretized with 200 cells ( $\Delta x = 0.01$ ). Because of the nonzero velocity of  $\vec{u} = 1$ , the RHS of the phase field equation is indeed not zero even at long times, resulting in a loss of Galilean invariance by the inconsistent models. All parameters and numbers in this section are dimensionless.

We consider three options for the phase field equation. The first option is the second-order conservative phase field model (Chiu & Lin 2011; Mirjalili *et al.* 2020),

$$\vec{R} = \gamma \left[ \epsilon \nabla \phi - \phi(1 - \phi) \frac{\nabla \phi}{|\nabla \phi|} \right], \quad (4.1)$$

where we use  $\gamma = |\vec{u}|$  and  $\epsilon = \Delta x$ . The second option is the standard Cahn-Hilliard equation,

$$\vec{R} = \gamma M(\phi) \nabla \mu, \quad (4.2)$$

where  $\mu$  is the chemical potential, defined as

$$\mu = \frac{4\phi(\phi - 1)(2\phi - 1)}{\epsilon} - \epsilon \nabla^2 \phi. \quad (4.3)$$

Here,  $\epsilon = 4\Delta x$  is our choice for the interfacial thickness parameter and  $\gamma = 3\epsilon^3$ . For the second phase field option, we use constant mobility,

$$M(\phi) = 1, \quad (4.4)$$

in accordance with traditional Cahn-Hilliard models. For the third option, we use degenerate mobility, given by

$$M(\phi) = 1 - (1 - \phi)^2. \quad (4.5)$$

#### 4.1. Test 1: confined scalar with a two-scalar model

In this test, we assess the consistency of the two-scalar model presented in Eqs. (2.8)–(2.9). We consider a two-phase system with a scalar confined in phase 1; that is,  $D_2 = 0$ . Since  $D_2 = 0$ , we have  $J = 0$ , allowing us to isolate the effect of the new terms. Figure 1 shows the phase field and concentration field for  $c_1$  at  $t = 0$ . We initialize the scalar concentrations with  $c_1(x, t = 0) = 3\phi(x, t = 0)$  and  $c_2(x, t = 0) = 0$ . It is clear that all the two-scalar models reduce to  $0 = 0$  for the  $c_2$  transport equation. As such,  $c_2$  is not plotted for this case. The analytical solution to this problem is  $c_1(x, t) = 3\phi(x, t)$  for all  $t > 0$ . This is independent of the value of the diffusion coefficient,  $D_1 = 0.4$ , as diffusion does not affect the scalar field when the local concentration ( $c_1/\phi$ ) is spatially uniform. Due to the constant imposed velocity of  $\vec{u} = 1$ , we have  $R \neq 0$ . Hence, this problem can assess the importance of consistently accounting for  $\vec{R}$  in scalar transport.

If we define the error for computations to be given by  $\text{error} = c_1(x, t) - 3\phi(x, t)$ , the errors for various scalar transport models and phase field equations are plotted in Figure 2 at  $t = 2$ , when the drop has returned to its initial position. By consistent, we refer to Eqs. (2.8)–(2.9); inconsistent 1 refers to Eqs. (2.8)–(2.9) without the last term; and inconsistent 2 refers to the use of Eqs. (2.12)–(2.13). Moreover, for the phase field equations, the results from the second-order phase field model [Eq. (4.1)] are shown in Figure 2(a,b), the constant mobility Cahn-Hilliard model [Eqs. (4.2)–(4.4)] results are shown in Figure 2(c,d), and the degenerate mobility Cahn-Hilliard model [Eqs. (4.2)–(4.3), and (4.5)] results are shown in Figure 2(e,f). Note that the results for the inconsistent 2 option are not displayed for the Cahn-Hilliard-based models because they suffered from significant leakage. This is due to the phase field equilibrium assumption used in deriving the first terms on the RHS of the inconsistent 2 model [Eqs. (2.12)–(2.13)], which, evidently, can be grossly invalid for models based on the Cahn-Hilliard equation.

According to the results, it is clear that the errors committed by the consistent model are on the order of machine precision, whereas for the inconsistent options, we see relatively large errors. It is also apparent from Figure 2(a,b) that even for the second-order phase field, the inconsistent 2 model used by Jain & Mani (2020) and Mirjalili *et al.* (2022) results in errors that are even larger than the inconsistent 1 model. This demonstrates how precarious the assumption of phase field equilibrium can be during the derivation of equations that are coupled to the phase field equations. Overall, Figure 2 also confirms that the consistent model’s performance is independent of the choice of phase field equation. Finally, we note that, considering the magnitude of the error, all the simulations used in Figure 2 prevented leakage of the scalar from the drop. This would not be possible using one-scalar models, even with the consistency correction given by Eq. (2.2).

#### 4.2. Test 2: moderate diffusivity ratio

This test assesses the effect of our consistency corrections for the one-scalar model [Eq. (2.2)] and the two-scalar model [Eqs. (2.8)–(2.9)]. Figure 3(a) shows the initial condition for the one-scalar simulations. We start the simulations with  $c(x, t = 0) = 3\phi(x, t = 0)$ , similar to the previous case. The drop is advected in the periodic domain with  $\vec{u} = 1$ . The diffusivities in the two phases are  $D_1 = 4$  and  $D_2 = 2$ , and  $K_{\text{eq}} = 5$ . As such, this is a case where an interphase transfer is expected. The solution from the consistent one-scalar model in Eq. (2.2) (denoted  $c_{\text{os,c}}$ ) and the inconsistent one-scalar model

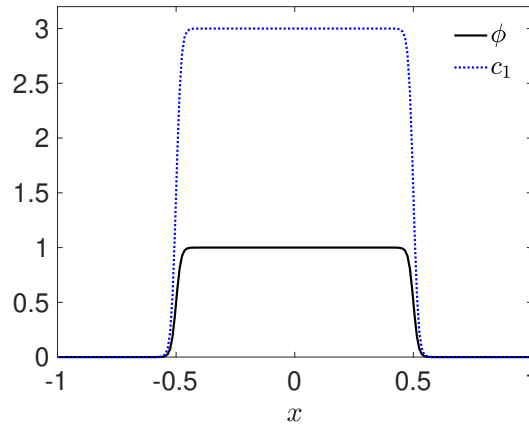


FIGURE 1. The initial condition for the phase field variable ( $\phi$ ) and the amount of scalar in phase 1 per total volume ( $c_1$ ) plotted as a function of space for Test 1.

given by omitting the last term (denoted  $c_{os, i}$ ) at  $t = 1$  and  $t = 2$  are shown in Figure 3(b,c). The solutions essentially show that as the scalar diffuses throughout both phases, the concentration attains a jump across the interface in accordance with  $K_{eq} = 5$ . While the inconsistent model seems to qualitatively produce accurate results, we can quantitatively assess its accuracy by examining  $T = c/K_{eff}$ , which can be thought of as the primitive variable that is continuous and constant at long times, that is, the chemical potential for mass transport or temperature for heat transport. For this problem, the steady-state value for this variable is  $T_{ss} = 2.5$ .

Figure 4 shows the errors in achieving the steady-state solution at  $t = 2$  for various phase field models and various scalar transport equations. Figure 4(a) shows errors from the one-scalar models coupled to the second-order phase field equation [Eq. (4.1)]. For the same phase field equation, Figure 4(b) shows errors from the consistent two-scalar model versus the inconsistent two-scalar model given by omitting the last terms on the RHS of Eqs. (2.8)-(2.9). Figure 4(c,d) is similar to Figure 4(a,b) in every aspect other than utilization of constant mobility Cahn-Hilliard equations [Eqs. (4.2)-(4.4)]. The consistent model results in errors below plotting accuracy while omitting the consistency correction always results in non-negligible errors. Moreover, while confirming that the consistency correction accounting for  $\bar{R}$  is needed regardless of the phase field model or choice of a one-scalar or two-scalar approach, it also shows that the other terms, including  $J$ , can model the interphase transfer and diffusion accurately for both phase field options. Based on the discussions in Section 2.2, this is expected because upon reaching thermodynamic equilibrium, regardless of the phase field equation, the two-scalar models attain steady and spatially uniform values for  $c_1/\phi = K_{eq}c_2/(1 - \phi) = 2.5$ . This causes the first two terms on the RHS of Eqs. (2.8)-(2.9) to vanish and renders these two equations continuously and discretely equivalent to (and consistent with) the phase field equation.

## 5. Conclusions

In this work, we presented consistent one-scalar and two-scalar models for the transport of passive scalars in simulations of two-phase flows with conservative phase field methods. In particular, we explained how the scalar transport equations should consis-

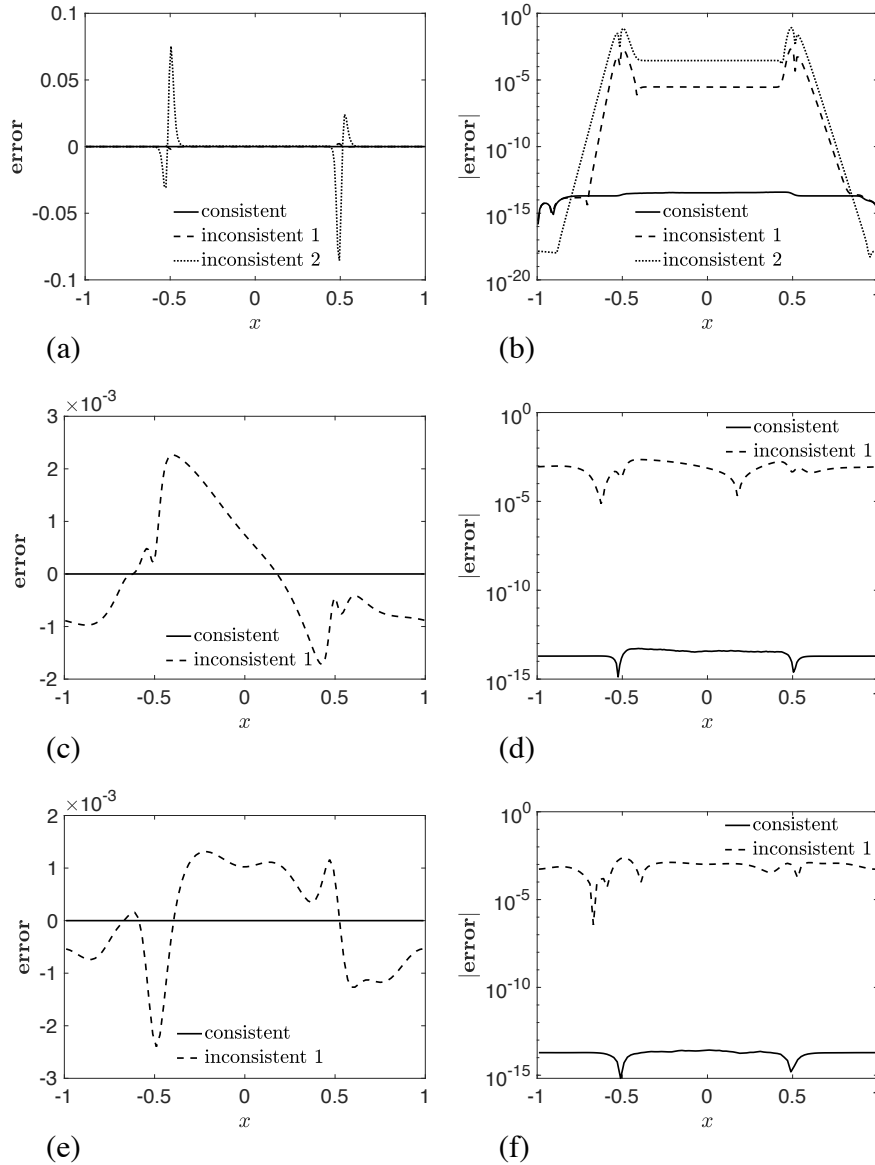


FIGURE 2. Errors for Test 1 at  $t = 2$  using consistent and inconsistent two-scalar models are compared for simulations performed with various phase field methods. (a, b) Errors for the second-order phase field model [Eq. (4.1)]. (c, d) Errors for the constant mobility Cahn-Hilliard model [Eqs. (4.2)-(4.4)]. (e, f) Errors for the degenerate mobility Cahn-Hilliard model [Eqs. (4.2)-(4.3) and (4.5)].

tently account for an out-of-equilibrium interface (i.e., non-zero fluxes in the RHS of the phase field equation). Crucially, the models presented are applicable to all conservative phase field methods, including second-order PDEs based on the Allen-Cahn equation and fourth-order PDEs based on the Cahn-Hilliard equation. We outlined the proof for the consistent models and briefly described the computational approach and requirements

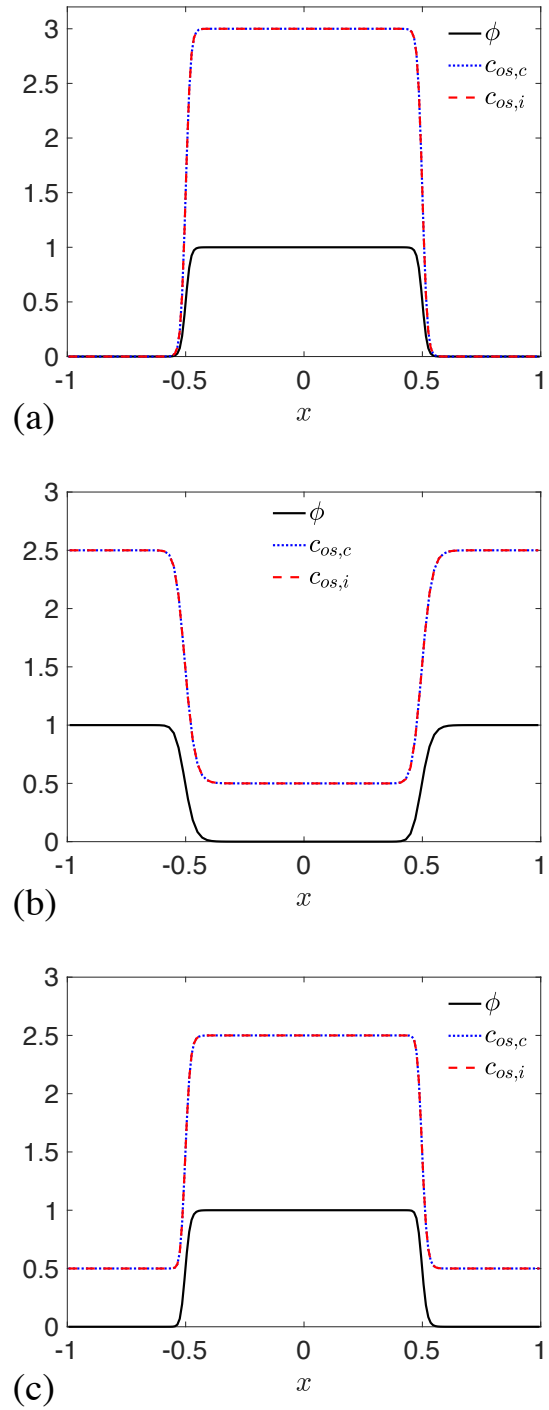


FIGURE 3. Evolution of the phase field variable and scalar values predicted by the one-scalar models for Test 2 at (a)  $t = 0$ , (b)  $t = 1$ , and (c)  $t = 2$ , when the solution has achieved a steady profile advecting in the  $x$  direction.

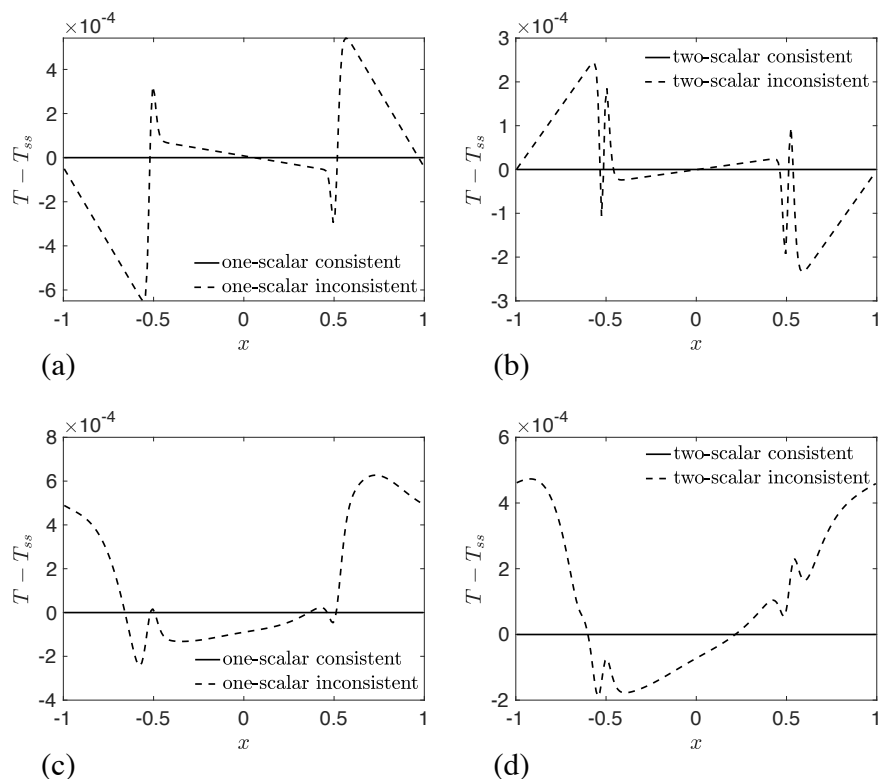


FIGURE 4. Errors for Test 2 at  $t = 2$  using consistent and inconsistent one-scalar and two-scalar models are compared for simulations performed using various phase field methods. (a, b) Errors for the second-order phase field model [Eq. (4.1)] for one-scalar and two-scalar models, respectively. (c, d) Errors for the constant mobility Cahn-Hilliard model [Eqs. (4.2)-(4.4)] for one-scalar and two-scalar models, respectively.

for positivity. We then used two simple numerical tests to verify that the PDE models are indeed consistent by comparing them to previous models and models that ignore the terms accounting for the RHS flux of the phase field equation.

In a future publication, we will formally derive the consistent models and prove the positivity criteria. Extensions to  $N$ -phase flows will be presented, and rigorous numerical testing in 2D and 3D flows will be carried out. Finally, we will couple the phase field and scalar transport equations to the momentum transport equation to solve practical problems of interest using various phase field methods.

### Acknowledgments

We acknowledge financial support from Palo Alto Research Center (grant 249996). We also thank Mr. Omkar Shende for helpful comments and suggestions.

### REFERENCES

ABELS, H., GARCKE, H. & GRÜN, G. 2012 Thermodynamically consistent, frame in-

- different diffuse interface models for incompressible two-phase flows with different densities. *Math. Mod. Meth. Appl. S.* **22**, 1150013.
- BOTHE, D. & FLECKENSTEIN, S. 2013 A volume-of-fluid-based method for mass transfer processes at fluid particles. *Chem. Eng. Sci.* **101**, 283–302.
- CHIU, P.-H. & LIN, Y.-T. 2011 A conservative phase field method for solving incompressible two-phase flows. *J. Comput. Phys.* **230**, 185–204.
- DAI, S. & DU, Q. 2016 Computational studies of coarsening rates for the Cahn-Hilliard equation with phase-dependent diffusion mobility. *J. Comput. Phys.* **310**, 85–108.
- DAVIDSON, M. R. & RUDMAN, M. 2002 Volume-of-fluid calculation of heat or mass transfer across deforming interfaces in two-fluid flow. *Numer. Heat Tr. B-Fund.* **41**, 291–308.
- FU, G. & HAN, D. 2021 A linear second-order in time unconditionally energy stable finite element scheme for a Cahn-Hilliard phase-field model for two-phase incompressible flow of variable densities. *Comput. Method. Appl. M.* **387**, 114186.
- HUANG, Z., LIN, G. & ARDEKANI, A. M. 2020 Consistent and conservative scheme for incompressible two-phase flows using the conservative Allen-Cahn model. *J. Comput. Phys.* **420**, 109718.
- HUANG, Z., LIN, G. & ARDEKANI, A. M. 2021 A consistent and conservative model and its scheme for N-phase-M-component incompressible flows. *J. Comput. Phys.* **434**, 110229.
- HUANG, Z., LIN, G. & ARDEKANI, A. M. 2022 A consistent and conservative phase-field model for thermo-gas-liquid-solid flows including liquid-solid phase change. *J. Comput. Phys.* **449**, 110795.
- JACQMIN, D. 1999 Calculation of two-phase Navier-Stokes flows using phase-field modeling. *J. Comput. Phys.* **155**, 96–127.
- JAIN, S. S. 2022 Accurate conservative phase-field method for simulation of two-phase flows. *J. Comput. Phys.* **469**, 111529.
- JAIN, S. S. & MANI, A. 2020 Modeling transport of scalars in two-phase flows with a diffuse-interface method. arXiv:2011.10705 [physics.flu-dyn].
- JAIN, S. S., MANI, A. & MOIN, P. 2020 A conservative diffuse-interface method for compressible two-phase flows. *J. Comput. Phys.* **418**, 109606.
- KHANWALE, M. A., LOFQUIST, A. D., SUNDAR, H., ROSSMANITH, J. A. & GANAPATHYSUBRAMANIAN, B. 2020 Simulating two-phase flows with thermodynamically consistent energy stable Cahn-Hilliard Navier-Stokes equations on parallel adaptive octree based meshes. *J. Comput. Phys.* **419**, 109674.
- LIU, J., LANDIS, C. M., GOMEZ, H. & HUGHES, T. J. 2015 Liquid–vapor phase transition: thermomechanical theory, entropy stable numerical formulation, and boiling simulations. *Comput. Method. Appl. M.* **297**, 476–553.
- MIRJALILI, S., IVEY, C. B. & MANI, A. 2019 Comparison between the diffuse interface and volume of fluid methods for simulating two-phase flows. *Int. J. Multiphas. Flow* **116**, 221–238.
- MIRJALILI, S., IVEY, C. B. & MANI, A. 2020 A conservative diffuse interface method for two-phase flows with provable boundedness properties. *J. Comput. Phys.* **401**, 109006.
- MIRJALILI, S., JAIN, S. S. & DODD, M. 2017 Interface-capturing methods for two-phase flows: an overview and recent developments. *Annual Research Briefs*, Center for Turbulence Research, Stanford University, pp. 117–135.

- MIRJALILI, S., JAIN, S. S. & MANI, A. 2022 A computational model for interfacial heat and mass transfer in two-phase flows using a phase field method. *Int. J. Heat Mass Tran.* **197**, 123326.
- MIRJALILI, S. & MANI, A. 2021 Consistent, energy-conserving momentum transport for simulations of two-phase flows using the phase field equations. *J. Comput. Phys.* **426**, 109918.
- SHEN, J. & YANG, X. 2010 A phase-field model and its numerical approximation for two-phase incompressible flows with different densities and viscosities. *SIAM J. Sci. Comput.* **32**, 1159–1179.
- SOLIGO, G., ROCCON, A. & SOLDATI, A. 2019 Coalescence of surfactant-laden drops by phase field method. *J. Comput. Phys.* **376**, 1292–1311.
- TEIGEN, K. E., LI, X., LOWENGRUB, J., WANG, F. & VOIGT, A. 2009 A diffuse-interface approach for modeling transport, diffusion and adsorption/desorption of material quantities on a deformable interface. *Commun. Math. Sci.* **4**, 1009–1037.
- YUE, P., FENG, J. J., LIU, C. & SHEN, J. 2004 A diffuse-interface method for simulating two-phase flows of complex fluids. *J. Fluid Mech.* **515**, 293–317.
- ZHENG, X., BABAEI, H., DONG, S., CHRYSOSTOMIDIS, C. & KARNIADAKIS, G. 2015 A phase-field method for 3D simulation of two-phase heat transfer. *Int. J. Heat Mass Tran.* **82**, 282–298.
- ZHU, G., KOU, J., YAO, B., WU, Y.-s., YAO, J. & SUN, S. 2019 Thermodynamically consistent modelling of two-phase flows with moving contact line and soluble surfactants. *J. of Fluid Mech.* **879**, 327–359.
- ZHU, G., KOU, J., YAO, J., LI, A. & SUN, S. 2020 A phase-field moving contact line model with soluble surfactants. *J. Comput. Phys.* **405**, 109170.